

Statistical investigation on firebrand behaviour in a simulated 3D fire whirl

Yuchen Zhang and Yang Zhang
Department of Mechanical Engineering, University of Sheffield
Sheffield, S1 3JD, UK

1 Abstract

The firebrands lofted by flow field is a vital mechanism of long-distance fire spread in the forest fire. Although many previous researches have been investigated the transportation of firebrands under the convective plume, few focused on the impact of fire whirl. The existence of a fire whirl will largely increase the maximum spotting distance, while researchers know little about its detailed physics. In this paper, a 3D fire whirl has been created by FDS, in order to study the effect of aerodynamic lift in the lofting mechanism of firebrands in fire whirl. By tracking each firebrand's trajectories, a relationship between the inclined angle to the maximum reachable height has been established. The trajectories that considered and ignored the impact of aerodynamic lift demonstrated that the aerodynamic lift's impact on the trajectories is significant. It suggests that the aerodynamic lift should be included in the prediction of firebrand lofting to improve the accuracy.

2 Introduction

Spotting ignition caused by lofted firebrands is a significant mechanism of fire spread. It leads to the creation of secondary fires by igniting the unburned fuel from lofted firebrands. Even today, the tragedies are still hard to avoid, from one mile to a half-mile spotting distance has been observed in the most recent Caldor Fire in California [6].

A huge amount of research has already been undertaken since Tarifa's research [1] in the 1960s. In the area of experiment, Manzello [2], who developed the Fire dragon as the device to study the transportation of firebrand, and other researchers presents plenty of investigations such as the property of secondary ignition and spotting distance under different flow conditions and different material. In the area of theoretical study, Muraszew [3] and other researchers have built various transportation models to predict and explain the phenomenon of spotting, which are under different flow conditions, different shapes of firebrands and different aerodynamic assumptions. Nevertheless, there are still some limitations that current studies are not fully covered. Among them, the lofting mechanism might be an important one. Muraszew [3] firstly suggested that most long-range firebrands are lofted by fire whirl, whereas short-range firebrands are mostly lofted by the convective plume, which is widely accepted by the later researchers [4]. However, little research has focused on the lofting mechanism of firebrands that are aloft by fire whirl. As the long-range firebrands

are more likely to fly over the barrier and caused disasters. It is essential to further analyse the detail physics in this situation.

In this paper, numerical simulation has been conducted to determine the trajectory of firebrands that are lofted by fire whirl at different incident angles. To introduce the flow condition of fire whirl, a widely-used open source LES simulation software, Fire Dynamic Simulator, has been utilized. The research focused on the effect of aerodynamic lift force during the lofting stage of firebrands. By calculating the trajectory with and without the aerodynamic lift force, the lift effects are discussed in detail.

3 Computational model

In this study, the large eddy simulation (LES) based on the fire field simulator, namely Fire Dynamics Simulator (FDS) ver 6.7.6 was utilised. A subgrid-scale turbulence model is implemented in FDS along with fully coupled combustion, radiation, and evaporation models to feasibly account for the fire phenomena. It solves numerically a Navier-stokes equation with a low Mach number approximation. An explicit second-order predictor-corrector scheme is adopted for calculating the variables such as velocity, pressure, and temperature.

1 Transport of firebrands

In the lofting stage of firebrands spotting phenomenon, a mathematical model for determining the trajectory and predicting the maximum potential spotting distance is developed. When the firebrand being released into the main fire whirl, it is mainly affected by the flow condition and supported by aerodynamic drag and lift forces. The coordinate system cannot be simplified as a two-dimensional assumption, as the fire whirl flow condition is not axisymmetric in spatial during the firebrand's transportation.

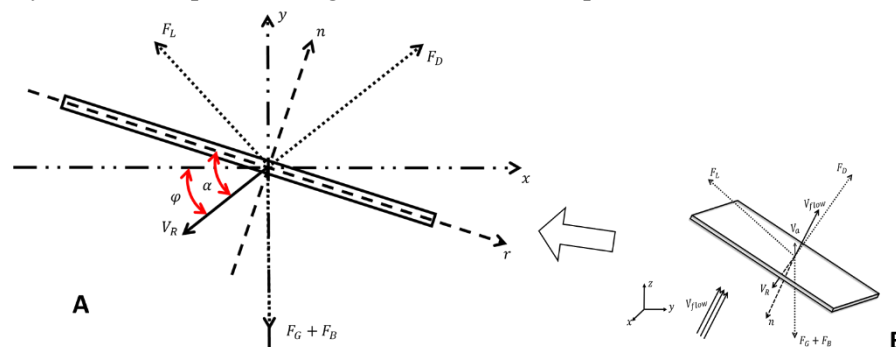


Figure 1. Schematic representations of the transporting model of a disk-shaped firebrand in a flow field. This numerical model is based on the following assumptions:

- 1) Firebrands are assumed to be released at a fixed position in the main fire zone. The ambient flow field due to the fire whirl is calculated by the Fire Dynamic Simulator (FDS)
- 2) Firebrands are idealized as rectangular-shaped disks and its areal density of firebrand is assumed to be $0.05 \text{ kg} / \text{m}^2$. It is assumed that relative velocity, the normal vector of the disk shape of firebrand and gravity to be coplanar.
- 3) The rotation and vibrations of the firebrand, such as tumbling and wobbling, are neglected.
- 4) The firebrand is assumed to be unburned during transportation. Thus, the shapes, size and mass of firebrands are kept unchanged during the propagation.
- 5) For simplicity of calculation, the velocity field generated by the fire whirl is assumed to be constant after the firebrand is released. To studying the impact of the aerodynamic lift effect, the solutions with and without the impact of lift were calculated by applying the same flow condition.

2 Aerodynamic forces

Aerodynamic forces exerted on the disk-shaped firebrand transporting inflow include the aerodynamic drag, F_D , lift, F_L , and the gravity combined with buoyancy, $F_G + F_B$. The net force on firebrand could be expressed as:

$$F = F_D + F_L + F_G + F_B$$

Where magnitude of F_D and F_L could be expressed as:

$$F_l = \frac{1}{2} C_l \cdot \rho \cdot V_r^2 \cdot A_{ref}$$

$$F_d = \frac{1}{2} C_d \cdot \rho \cdot V_r^2 \cdot A_{ref}$$

Where A_{ref} represents the firebrand's reference area. C_l and C_d represent the lift coefficient and drag coefficient, which are related to the firebrand's shape, angle of attack, and the Reynolds number of the system. V_r represents the relative velocity of the firebrand to the surrounding flow. ρ is the density of the surrounding air.

From the FDS's simulation result, it is known that the Reynolds number in this experiment is about 1046. For this relatively low Reynolds number, the formula for lift and drag coefficient for disk shape objects given in Zastawny are used [5].

The direction of the aerodynamic drag is always opposite to the relative velocity. Moreover, the aerodynamic lift's direction is always perpendicular to the relative velocity. And its direction vector could be express as:

$$n_{F_L} = \frac{n_{firebrand} \times (V_r \times n_{firebrand})}{|n_{firebrand} \times (V_r \times n_{firebrand})|}$$

The direction of the cross product could be measured by the right-hand rule. Therefore, in Figure 1, the right-hand coordinates is also been applied.

Similarly, the angle of attack could also be measured by:

$$\begin{cases} \alpha = \pi - \arccos\left(\frac{V_r \cdot n_{firebrand}}{|V_r|}\right) & \text{if } \alpha > \frac{\pi}{2} \\ \alpha = -\arccos\left(\frac{V_r \cdot n_{firebrand}}{|V_r|}\right) & \text{if } \alpha < 0 \\ \alpha = \arccos\left(\frac{V_r \cdot n_{firebrand}}{|V_r|}\right) & \text{otherwise} \end{cases}$$

3 Equation of the motion

Trajectories of the firebrands are determined from Newton's second law of motion as:

$$M \cdot \frac{dV}{dt} = F_D + F_L + F_G + F_B$$

By decomposing the vectors into x, y and z axes, newton's second law could be written as:

$$M \cdot \frac{dV_x}{dt} = \underbrace{\frac{1}{2} C_d \cdot \rho \cdot A_{ref} \cdot V_r \cdot V_{rx}}_{\text{Drag}} + \underbrace{\frac{1}{2} C_l \cdot \rho \cdot V_r^2 \cdot A_{ref} \cdot (n_{F_L} \cdot n_x)}_{\text{Lift}}$$

$$M \cdot \frac{dV_y}{dt} = \underbrace{\frac{1}{2} C_d \cdot \rho \cdot A_{ref} \cdot V_r \cdot V_{ry}}_{\text{Drag}} + \underbrace{\frac{1}{2} C_l \cdot \rho \cdot V_r^2 \cdot A_{ref} \cdot (n_{F_L} \cdot n_y)}_{\text{Lift}}$$

$$M \cdot \frac{dV_z}{dt} = \underbrace{\frac{1}{2} C_d \cdot \rho \cdot A_{ref} \cdot V_r \cdot V_{rz}}_{\text{Drag}} + \underbrace{\frac{1}{2} C_l \cdot \rho \cdot V_r^2 \cdot A_{ref} \cdot (n_{F_L} \cdot n_z)}_{\text{Lift}} + \underbrace{(\rho_f - \rho_a) \cdot V \cdot g}_{\text{Gravity and Bouyancy}}$$

4 Result and Discussions

In order to determine the effects of the fire whirl on the lofting performance of the unburning platform firebrands, the trajectory of firebrands that considering the aerodynamic lift effect has been calculated to compare with those neglecting the aerodynamic lift effect.



Figure 2. (a) Physical structure of two half-cylindrical walls of the fire whirl boundary. (b) Size of the fuel pool that is being utilized to generate the fire whirl.

The domain size is $0.275\text{m} \times 0.275\text{m} \times 0.8\text{m}$ with a grid resolution $60 \times 60 \times 150$ in x, y, and z directions. The fuel, ethanol vapour, which is generated by the evaporation of the liquid ethanol, has been used in the simulation. As it has been fully validated by previous research, its parameter shows below.

Table 1: Key parameters applied in simulation.

Liquid ethanol		Ethanol vapour	
Density	787 kg/m ³	Critical Flame Temperature	1427 °C
Specific Heat	2.45 KJ/(Kg*K)	Energy release per unit mass oxygen	1.31×10^4 kJ/kg
Conductivity	0.17 W/(m*K)	CO Yield	0.001
Emissivity	1.0	Soot Yield	0.008
Absorption Coefficient	40.0 1/m	Hydrogen Fraction	0.1
Boiling Temperature	76.0 °C		
Heat of vaporization	880 kJ/kg		

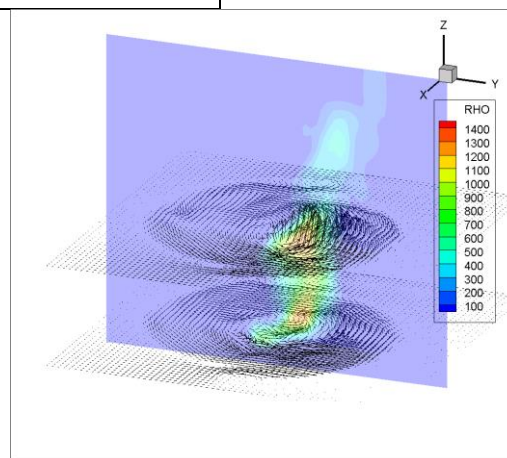


Figure 3. Vector field of velocity and contour plot of the temperature of fire whirl on different slices.

By comparing the impact of the aerodynamic lift effect to the trajectory of the firebrands. A group of the calculation has been achieved under the same flow condition. By controlling the same initial position, the same size of firebrands, and the same flow condition. The only variable that took into account in this study is the initial angle of inclination of the firebrands during transportation. Figure 4 shows a great different tendency on varying the trajectory of the firebrands in different initial inclined angles.

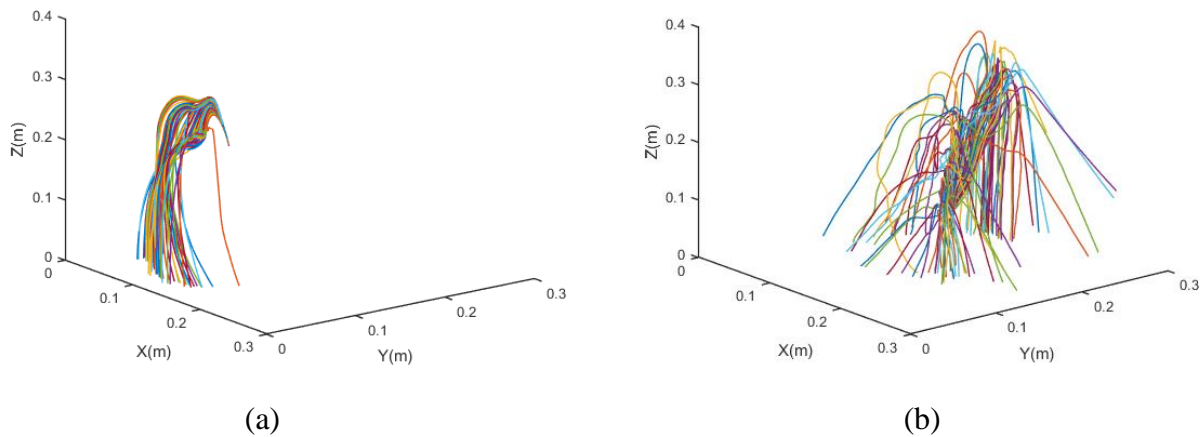


Figure 4. Trajectories of the firebrands that travelling in the velocity field shows in Figure 3. (a) shows the result that neglect the impact of aerodynamic lift. (b) shows the result that considering the impact of aerodynamic lift. All of the firebrands are released at the highest Z-axis velocity's position. Figure 4(a) shows the result of the trajectories that only considering the buoyancy, gravity, and aerodynamic drag effects. Comparing with Figure 4 (b) the trajectories only changed slightly at the beginning due to the varying of the angle of inclination. Starting with a tiny initial difference, a firebrand's trajectories can land at a different position.

Figure 4(b) shows the result that the trajectories varied significantly due to a slight change of the initial inclination angle. At some special angles, the trajectories are apparently different from the others. And the reached height is also higher than the others. By observing, it is clear that in Figure 4(a), the reached height is about 0.25m, which is about double the initial position. However, in Figure 4(b), the highest reachable height is more than 0.3m. Moreover, by comparing the landing position between Figure 4(a) and Figure 4(b), it is also clear that aerodynamic lift will increase the range of landing positions.

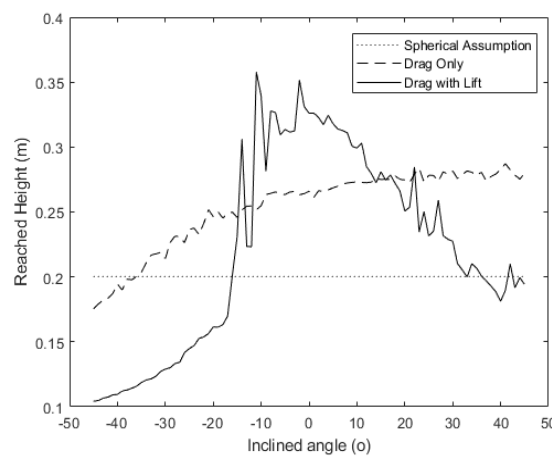


Figure 5. Comparing the highest reachable height in different initial inclination angles, that considering the aerodynamic lift, neglecting the aerodynamic lift, and in spherical equivalent assumption.

By tracking each firebrand with a different initial inclination angle, and list the highest reachable height. From Figure 5, it is clear that including the aerodynamic lift will significantly change the result of the trajectories. Within a short range of the inclination angle, the firebrand's reachable height has been increased significantly compared with the result from neglecting the impact of aerodynamic lift. While in the other angle, the aerodynamic lift shows a negative impact on the height that the firebrand could reach. In other words, the highest reachable height could be used to estimate the dangerousness of that firebrand introduced spotting fire.

5 Conclusion

This paper presented a systematic study on the lofting mechanism of firebrands lofted by simulated fire whirl. The LES simulation has been applied to generate the velocity field for the calculation of the trajectory of firebrands.

For the purpose of studying the impact of aerodynamic lift on the lofting of the firebrand, two groups of the ODE simulation has been calculated to quantify the differences. And the main conclusion is listed as follows:

- The aerodynamic lift effect has a significant effect on the lofting mechanism of firebrands under the fire whirl.
- The aerodynamic lift is not always the positive factor that boosts up the highest reachable height of firebrands. In some conditions, it will be a negative factor that makes the firebrand drop faster.

6 References

- [1] C. Sánchez Tarifa, P. Pérez Del Notario, F. García Moreno (1965), On the flight paths and lifetimes of burning particles of wood, in: Symp. Combust., [https://doi.org/10.1016/S0082-0784\(65\)80244-2](https://doi.org/10.1016/S0082-0784(65)80244-2).
- [2] Samuel L. Manzello, Sayaka Suzuki,(2013) Experimentally Simulating Wind Driven Firebrand Showers in Wildland-urban Interface (WUI) Fires: Overview of the NIST Firebrand Generator (NIST Dragon) Technology, *Procedia Engineering*, 62(2013) ,pp. 91-102, <https://doi.org/10.1016/j.proeng.2013.08.047>.
- [3] A. Muraszew, J.B. Fedele, W.C. Kuby, Trajectory of firebrands in and out of fire whirls, *Combust. Flame*. 30 (1977). [https://doi.org/10.1016/0010-2180\(77\)90081-5](https://doi.org/10.1016/0010-2180(77)90081-5).
- [4] E. Koo, P.J. Pagni, D.R. Weise, J.P. Woycheese, Firebrands and spotting ignition in large-scale fires, *Int. J. Wildl. Fire*. 19 (2010). <https://doi.org/10.1071/WF07119>.
- [5] Zastawny, M. , Mallouppas, G. , Fan, Z. , & Wachem, B. V. . (2012). Derivation of drag and lift force and torque coefficients for non-spherical particles in flows. *International Journal of Multiphase Flow*, 39(1), 227-239. <https://doi.org/10.1016/j.ijmultiphaseflow.2011.09.004>
- [6] capradio.org (2021). *Caldor Fire Updates: Fire Officials Don't See 'Any Major Threats' As Highway 88 Reopens, More Evacuations Lift*. Available from: <https://www.capradio.org/articles/2021/09/16/caldor-fire-latest-updates/> (Accessed at: 17th September 2021)